Published in final edited form as:
*Clin Cancer Res*. 2014 May 15; 20(10): 2783–2792. doi:10.1158/1078-0432.CCR-13-2364.

# Population Pharmacokinetics of Bevacizumab in Children with Osteosarcoma: Implications for Dosing

**David C. Turner**[1], **Fariba Navid**[2,3], **Najat C. Daw**[4], **Shenghua Mao**[5], **Jianrong Wu**[5], **Victor M. Santana**[2,3], **Michael Neel**[6], **Bhaskar Rao**[6], **Jennifer Reikes Willert**[7], **David M. Loeb**[8], **K. Elaine Harstead**[1], **Stacy L. Throm**[1], **Burgess B. Freeman III**[9], and **Clinton F. Stewart**[1,*]

[1]Department of Pharmaceutical Sciences, St. Jude Children's Research Hospital, Memphis, TN 38105, USA

[2]Department of Oncology, St. Jude Children's Research Hospital, Memphis, TN 38105, USA

[3]Department of Pediatrics, College of Medicine, University of Tennessee Health Science Center, Memphis, TN 38163, USA

[4]Division of Pediatrics, MD Anderson Cancer Center, Houston, TX 77030, USA

[5]Department of Biostatistics, St. Jude Children's Research Hospital, Memphis, TN 38105, USA

[6]Department of Surgery, St. Jude Children's Research Hospital, Memphis, TN 38105, USA

[7]Department of Pediatrics, Stanford School of Medicine, Palo Alto, CA 94304 USA

[8]Department of Oncology, Division of Pediatric Oncology, Sidney Kimmel Comprehensive Cancer Center at Johns Hopkins, Baltimore, MD 21231, USA

[9]Preclinical Pharmacokinetic Shared Resource, St. Jude Children's Research Hospital, Memphis, TN 38105, USA

## Abstract

**Purpose—**To describe sources of interindividual variability in bevacizumab disposition in pediatric patients and explore associations among bevacizumab pharmacokinetics and clinical wound healing outcomes.

**Experimental Design—**Prior to tumor resection, three doses of bevacizumab (15 mg/kg) were administered to patients (median age 12.2 years) enrolled on a multi-institutional osteosarcoma trial. Serial sampling for bevacizumab pharmacokinetics was obtained from 27 patients. A population pharmacokinetic model was fit to the data, and patient demographics and clinical chemistry values were systematically tested as predictive covariates on model parameters. Associations between bevacizumab exposure and wound healing status were evaluated by logistic regression.

**Results—**Bevacizumab concentration-time data were adequately described by a two-compartment model. Pharmacokinetic parameter estimates were similar to those previously reported in adults with a long median (range) terminal half-life of 12.2 days (8.6 to 32.4 days) and

[*]Clinton F. Stewart, Pharm.D. Department of Pharmaceutical Sciences, St. Jude Children's Research Hospital, 262 Danny Thomas Place, Memphis TN 38105 Telephone: (901) 595-3665; FAX: (901) 525-6869 clinton.stewart@stjude.org.

a volume of distribution indicating confinement primarily to the vascular space,49.1 mL/kg (27.1 to 68.3 mL/kg). Body composition was a key determinant of bevacizumab exposure as body mass index percentile was significantly ($p<0.05$) correlated to body-weight normalized clearance and volume of distribution. Furthermore, bevacizumab exposure prior to primary tumor resection was associated with increased risk of major wound healing complications after surgery ($p<0.05$).

**Conclusion—**A population pharmacokinetic model for bevacizumab was developed which demonstrated that variability in bevacizumab exposure using weight-based dosing is related to body composition. Bevacizumab dosage scaling using ideal body weight would provide an improved dosing approach in children by minimizing pharmacokinetic variability and reducing likelihood of major wound healing complications.

### Keywords

Bevacizumab; Population pharmacokinetics; Wound healing; Pediatric cancers; Angiogenesis inhibitors:endogenous and synthetic

## Introduction

Bevacizumab is a humanized monoclonal IgG1 antibody that inhibits vascular endothelial growth factor (VEGF), blocking its interaction with VEGF cell-surface receptors and the subsequent intracellular signaling cascade that promotes proliferation and mobilization of endothelial cells that comprise the tumor vasculature network (1). Preclinical data from xenograft studies suggest that single-agent therapy with bevacizumab impairs tumor growth in a variety of different tumor types (2), and the combination of bevacizumab with other cytotoxic agents or radiation therapy achieves additive or synergistic tumor growth inhibition (2-4). In clinical trials, bevacizumab has shown activity against colorectal cancer (5-10), non-small cell lung cancer (11), renal cell carcinoma (12), ovarian cancer (13), and glioblastoma multiforme (14-16). Based on data linking higher VEGF expression levels with poor prognosis and increased risk of metastases in osteosarcoma patients (17-19), we prospectively evaluated the feasibility a novel treatment regimen that combines standard chemotherapy with bevacizumab (Clinical trial NCT00667342).

The pharmacokinetic disposition of bevacizumab has been previously described in adult patients receiving dosages of 1–20 mg/kg every 1, 2, or 3 weeks (20, 21). The estimated terminal half-life in this patient population was 22.8 days (range, 13–45 days), consistent with other IgG-like antibodies. A Children's Oncology Group (COG) Phase I trial was recently conducted where bevacizumab was administered intravenously (5, 10, or 15 mg/kg) every 2 weeks to children with refractory solid tumors; however, pharmacokinetic evaluation was limited to non-compartmental analysis of data from only eight patients (22). Hence, the potential sources of interindividual variability of bevacizumab disposition in pediatric patients and the implications of this variability upon bevacizumab safety and efficacy remain poorly understood.

One major concern with adding bevacizumab to a treatment regimen for patients with osteosarcoma is that aggressive surgery is an integral part of curative therapy. Data suggest that bevacizumab administration could impede surgical wound healing, owing to the

underlying similarities between pathological angiogenesis and normal wound repair (23-27). Patients undergoing major surgical procedures who receive bevacizumab have an increased risk of postoperative bleeding and wound complications vs. patients receiving the same chemotherapy without bevacizumab (5, 28). Reported healing complications include abnormal bruising/bleeding and wound dehiscence (8, 28). Since these data suggest a link between bevacizumab treatment and wound healing complications, one of the key objectives of our trial was to establish whether a significant relationship exists between bevacizumab pharmacokinetic disposition and clinical wound healing outcomes. To address this, we performed intensive serial sampling for bevacizumab pharmacokinetics to define the pharmacokinetic parameters and interindividual variability of bevacizumab disposition in pediatric patients. We then examined the contribution of various patient covariates towards the interindividual variability of bevacizumab pharmacokinetic parameters and investigated the potential relationship between bevacizumab systemic exposure and postoperative wound complications.

## Patients and Methods

### Patient Population and Bevacizumab Administration

This study was carried out as part of a multi-institutional clinical trial (NCT00667342) to evaluate the feasibility of combining bevacizumab with chemotherapy for treatment of children with newly-diagnosed osteosarcoma. The trial was approved by the Institutional Review Board of each participating institution, and written informed consent was obtained from patients, parents, or legal guardians. Patients with either localized or metastatic osteosarcoma were eligible. Preoperative chemotherapy consisted of cisplatin (60 mg/m$^2$ days 1 and 2) and doxorubicin (25 mg/m$^2$ days 1-3) at weeks 0 and 5 and high-dose methotrexate (12 g/m$^2$ day 1) at weeks 3, 4, 8, and 9 (29). Bevacizumab was administered at 15 mg/kg IV three days prior to the first dose of chemotherapy at week 0 and on day 1 of week 3 and 5 of chemotherapy. Surgery for resection of the primary tumor was performed at approximately week 10. The first bevacizumab dose was infused over 90 minutes and if tolerated, subsequent doses were infused over 60 minutes and then 30 minutes. After surgery, bevacizumab was held for at least 5 weeks or until adequate wound healing occurred. Patients with localized disease continued on a regimen of cisplatin, doxorubicin and methotrexate whereas patients with metastatic disease also received ifosfamide and etoposide.

### Pharmacokinetic Sampling Strategy

Ten serial blood samples (2 mL each) for pharmacokinetic studies were collected with the first (week 0) and third (week 5) bevacizumab doses each at the following times: pre-dose, end of infusion, and at hours 1, 3, 6, 24 (± 4 hours), 48 (± 6 hours), 96 (±6 hours), 144 (± 24 hours), and 288 hours (± 24 hours) after the end of the infusion. Two blood samples were also collected with the second (week 3) bevacizumab dose both before and at the end of the infusion. After the third bevacizumab dose on week 5, samples were collected weekly until definitive surgery at week 10.

Twenty seven patients were assessable for bevacizumab pharmacokinetics. Of these, all had bevacizumab concentration-time data for weeks 0, 3, and 5 except one patient whose week 0 and week 3 dose was withheld (only week 5 administered). In total, 26 patients were studied on all three planned pre-surgery bevacizumab dosing occasions to define the interocassion variability of bevacizumab.

Blood samples were collected in a clot activator containing vacutainer tube that was placed upright to clot at room temperature (~30 minutes) then centrifuged for 10 minutes at 4°C at 3000×g. Extracted serum was stored at -80°C. Serum bevacizumab concentrations were determined using a proprietary GLP compliant, validated enzyme-linked immunosorbent assay (20) (QPS; Groningen, The Netherlands). All samples were analyzed as a single batch. The lower limit of sensitivity of this assay was 78 ng/mL.

## Population Pharmacokinetic Modeling

In total, concentration data from 749 serum samples were used for the population pharmacokinetic analysis. No samples other than the day 1 pre-infusion samples were below the lower limit of quantitation. The pharmacokinetic parameters of bevacizumab were determined by nonlinear mixed-effects modeling via NONMEM (version 7.2), sequentially using the Iterative Two Stage (ITS), Stochastic Approximation Expectation-Maximization (SAEM), and Importance Samping (IMP) estimation methods. Bevacizumab concentration-time profiles followed a bi-exponential decay (Supplementary Figure 1 and Supplementary Figure 2), so the data were fit by a two-compartment structural model with first-order elimination from the central compartment (ADVAN6 subroutine) as also described in previously published pharmacokinetic studies (20). The slope of the terminal elimination phase, β, was calculated using the *post hoc* micro-rate constants, and β was used to determine the terminal half-life, $t_{1/2}=\frac{ln\,(2)}{\beta}$.

The entire population was used to estimate population means and coefficients of variation of the bevacizumab central compartment volume of distribution ($V_{\text{normalized}}$ in mL/kg or $V_{\text{non-normalized}}$ in mL), total systemic clearance (CL in mL/day/kg), and intercompartmental rate constants between the central and peripheral compartment ($k_{12}$ and $k_{21}$ in $days^{-1}$). Interindividual variability (IIV) was assumed to be log-normally distributed for all pharmacokinetic parameters, so IIV was exponentially scaled on each population parameter. Thus, for the *i*th individual:

$$\theta_{i,k}=\theta_{Pop,k}\times \mathrm{e}^{\left(\sum_{\mathrm{j}=1}^{\mathrm{n}}\eta_{i,j,k}^{\theta}+\eta_{i,k}\right)} \quad \text{Equation 1}$$

where $\theta_{i,k}$ is the value of parameter, *k*, in the given individual, $\theta_{Pop,k}$ is the typical value of the parameter in the population, and $\eta_{i,k}$ is a normally distributed random variable with a mean of zero and a variance of $\omega^2$ (estimated by NONMEM). Since bevacizumab was administered on multiple occasions per individual, $\eta_{i,j,k}^{\theta}$ represents the variability of occasion j from individual i average value (i.e., between-occasion variability) with mean 0 and variance $ø^2$. An occasion was defined as the time from the start of the corresponding infusion to the start of the next infusion (or surgery). The full covariance matrix was

implemented with all between subject eta terms. The random-effect residual error model, resulting from assay errors and other unexplained sources, was described by mixed proportional plus additive terms:

$$c_{i,m}=c_{predicted,i,m}\times(1+\varepsilon_{prop,i,m})+\varepsilon_{add,i,m} \quad \text{Equation 2}$$

in which $C_{i.m}$ is the *m*th measured concentration of the *i*th individual, $c_{predicted,i,m}$ is the corresponding predicted concentration and $\varepsilon_{\text{prop},i,m}$ and $\varepsilon_{\text{add},i,m}$ are the normally distributed proportional and additive random variables with mean zero and variances $\sigma^2_{\varepsilon_p}$ and $\sigma^2_{\varepsilon_a}$.

A bootstrap resampling method (n=1,000) was applied for internal validation of the final population model. Lastly, a visual predictive check (VPC) was employed to evaluate the adequacy of the final population model by comparing the distribution of observed concentrations with the distribution of simulated concentrations based on the final estimates of parameter/covariate relationship.

## Relationship Between Pharmacokinetic Parameters and Covariates

The following exploratory covariates were tested to explain the interindividual variability of the population pharmacokinetic model: age, gender, height (HT), total body weight (TBW), ideal body weight (IBW), adjusted body weight (AIBW), body mass index percentile (BMI %), body surface area (BSA) calculated using the Gehan and George formula (30) using TBW and HT, serum albumin, total protein, alkaline phosphatase (ALKP), and aspartate aminotransferase (AST). For modeling purposes, measurements were taken at baseline prior to the first bevacizumab infusion. The $\chi^2$ test was used to compare the objective function values (OFV) of nested models (likelihood ratio test). A covariate was considered significant in this analysis if the addition of the covariate to the model reduced the -2 log-likelihood at least 3.84 units ($P < 0.05$, based on the $\chi^2$ test for the difference in the -2 log-likelihood between two hierarchical models that differ by 1 degrees of freedom).

BMI was calculated as TBW (kg) divided by $HT^2$ ($m^2$). IBW and BMI% were determined using the gender-specific BMI-for-age growth charts established for children 2-20 years of age published by the Center for Disease Control and Prevention (31). According to these standard guidelines, BMI values characterized in the upper 15$^{th}$ percentile are classified as overweight while a child is considered underweight when the BMI is less than the 5$^{th}$ percentile for age and gender. AIBW was calculated using IBW and TBW by the conventional formula, $AIBW = (TBW - IBW) \times 0.40 + IBW$. Clinical studies suggest the weighting factor of 0.40 in this formula is appropriate because extracellular water space in adipose tissue is approximately 40% that of other tissues (32-35).

Three different parameterizations were explored to describe the relation between TBW and bevacizumab pharmacokinetic parameters:

$$\boldsymbol{Model\ parameterization}\,[\boldsymbol{A}]\text{:}\begin{cases}\theta_{Pop,CL} = \left(\theta_{base,CL}\right)\times TBW^{0.75}\\ \theta_{Pop,V} = \left(\theta_{base,V}\right)\times TBW^{1.0}\end{cases}$$

$$\boldsymbol{Model\ parameterization}\,[\boldsymbol{B}]\text{:}\begin{cases}\theta_{Pop,CL} = \left(\theta_{base,CL}\right)\times TBW\\ \theta_{Pop,V} = \left(\theta_{base,V}\right)\times TBW\end{cases}$$

$$\boldsymbol{Model\ parameterization}\,[\boldsymbol{C}]\text{:}\begin{cases}\theta_{Pop,CL} = \theta_{base,CL}\\ \theta_{Pop,V} = \theta_{base,V}\end{cases}$$

In model parameterization [A], body weight was implemented *a priori* as a covariate for clearance and volume of distribution values using an allometric equation with fixed exponent of 0.75 for clearance and 1.0 for volume of distribution. In parameterization [B], a fixed linear relationship between TBW and clearance as well as TBW and volume of distribution was assumed because bevacizumab dosages on this protocol were scaled based on patient weight (this relation to body weight is inherently built into all bevacizumab TBW-based clinical dosing regimens). In the third parameterization, [C], no *a priori* relation between body weight and bevacizumab pharmacokinetic parameters was presumed.

As a preliminary investigation of associations between other potential covariates (aside from TBW) and model parameters, scatter plots of the covariates and post-hoc parameter estimates were visually examined. All covariates in this screening process were tested in a univariate fashion in the population model by inclusion in the model as an additional estimated parameter. The relationship between the pharmacokinetic parameters and categorical or continuous covariates (aside from TBW) were described using either a simple multiplicative or an exponential multiplicative model. The exponential multiplicative model codes for a fractional change in the parameter estimate and avoids issues with negative parameter values during covariate effect estimation. Thus, for the exponential multiplicative model, the population estimate $\theta_{Pop,k}$ of parameter *k* was determined according to the following fixed-effect relationship:

$$\theta_{Pop,k}=\theta_{base,k}\times e^{covariate_p\times\theta_{p,k}} \quad \text{Equation 3}$$

where $\theta_{base,k}$ represents the baseline population parameter estimate not explained by any of the included covariates, and $\theta_{p,k}$ was the effect of covariate *p* on the model parameter, *k*. Likewise, the simple multiplicative model was coded according to the relationship in equation 4:

$$\theta_{Pop,k}=\theta_{p,k}\times Covariate_p \quad \text{Equation 4}$$

For evaluation of the predictive performance of the models, clearance and $V_{non\text{-}normalized}$ were calculated for each patient, given the model fixed effects relationships. The prediction error ($P_e$) for individual parameter estimate was calculated as the population prediction, $k_{POP,I}$ minus the *post hoc* parameter estimate $k_{posthoc,i}$ expressed as a relative percentage of the *post hoc* estimate:

$$P_e = \frac{k_{POP,i} - k_{posthoc,i}}{k_{posthoc,i}} \times 100\% \quad \text{Equation 5}$$

Predictive performance of each model was then assessed by the relative mean prediction error (%MPE) as a measure of parameter estimation bias and the relative root mean square prediction error (RMSE%) as a measure of precision:

$$\%MPE = \frac{\sum P_e}{n} \quad \text{Equation 6}$$

$$RMSE\% = \sqrt{\frac{\sum P_e^2}{n}} \quad \text{Equation 7}$$

### Assessment of Pharmacokinetic/Pharmacodynamic Relationship

The relation of bevacizumab area under the concentration-time curve (AUC) and wound healing complications was investigated because AUC is the best metric of the overall systemic exposure of bevacizumab. Cumulative bevacizumab AUCs were calculated in NONMEM by integrating model predicted bevacizumab serum concentrations using a dummy compartment. AUC was calculated from the start of infusion of the first dose to the beginning of the second infusion on week 3 ($AUC_{0–3}$), from the start of infusion of the first dose to beginning of the third infusion at week 5 ($AUC_{0–5}$) and from the beginning of the third infusion at week 5 to surgery ($AUC_{5–surgery}$).

### Statistical Analysis

Wound healing status was represented as a nominal dependent variable with two possible values (e.g., yes or no), while AUC data were treated as a continuous independent variable. A univariate logistic model was applied to evaluate the association between bevacizumab systemic exposure and wound healing status. A *p* value of 0.05 was chosen as the a priori cutoff significance level.

## Results

### Patient Characteristics

Bevacizumab pharmacokinetic studies were evaluable in twenty seven patients all of which had bevacizumab concentration-time data for weeks 0, 3, and 5 except one patient whose week 0 and week 3 dose was withheld (only week 5 administered). The median (range) time from the last bevacizumab dose to surgery was 7.3 weeks (5.9 to 9.3). The patients' baseline characteristics are summarized in Table 1.

### Population Pharmacokinetic Modeling

As described in the Methods section, three model parameterizations were explored to describe the relation between TBW and bevacizumab pharmacokinetic parameters. To facilitate comparison to prior published TBW-normalized bevacizumab pharmacokinetic

data and also emphasize dependency of bevacizumab exposure on body composition in children in this report, we have elected to summarize our analysis of model parameterization [B] (fixed linear relation between TBW and CL/ TBW and V). Comparison of all model parameterizations are presented in text below and summary results of this assessment are also provided in Supplementary Table 1.

Initial diagnostic plots for the parameterization [B] base population pharmacokinetic model are shown in Figs. 1A and 1B. The individual predicted concentrations were symmetrically distributed around the line of identity. Conditional weighted residual values were symmetrical and generally distributed around zero. No bias was apparent in the plot of the predicted concentration versus the conditional weighted residual (not shown), suggesting an adequate structural model. Median (range) individual post-hoc CL, $V_{normalized}$, $k_{12}$, and $k_{21}$ estimates were 4.8 mL/day/kg (2.4 to 7.5), 49.1 mL/kg (27.1 to 68.3), 0.22 $days^{-1}$ (0.12 to 0.32), and 0.34 $days^{-1}$ (0.07 to 0.67), respectively.

Independent covariate searches for each model parameterization identified BMI% as a significant covariate for both parameterizations [A] and [B], i.e., those models containing *a priori* fixed TBW relationships for clearance or volume of distribution. Diagnostic plots generated from the pharmacokinetic model for parameterization [B] with BMI% as a covariate on CL and $V_{normalized}$ confirmed that the negative bias from the line of unity in the population prediction versus observed concentration (Fig. 1C) was improved after accounting for interpatient differences in BMI% (Fig. 1D). The population parameter estimates from the final model bootstrap for parameterization [B] in Table 2 indicate that all final pharmacokinetic parameters for model parameterization [B] were precisely estimated, with relative standard errors (RSEs) of <7%. Monte Carlo simulations performed with the final covariate-containing model for parameterization [B] (Supplementary Figure 3), indicate the population model successfully captured the distribution of observed bevacizumab serum concentrations by accounting for body composition in the model.

Inclusion of BMI% to correct bias introduced by *a priori* fixed TBW relationships underscores the dependency of bevacizumab inter-individual variability on body composition when administered on a linear TBW-based clinical regimen and furthermore confirms TBW to be a suboptimal body size descriptor for bevacizumab pharmacokinetics in children. This hypothesis is also supported by subsequent covariate analyses of model parameterization [C] indicating bevacizumab CL and $V_{non\text{-}normalized}$ scale linearly with IBW in children, rather than TBW (Figs. 2 and 3). Precision and bias of population parameter estimates for parameterizations [A], [B], and [C] (with IBW), summarized in Supplementary Table 1, suggest linear IBW relationship accounts for a greater proportion of the interindividual variability in children than either of the TBW fixed effects in [A] or [B]. The net change in OFV of model parameterization [C] after inclusion of IBW (ΔOFV = - 62.4) was significantly greater than the ΔOFV comparing base parameterization [C] to [B] (ΔOFV = - 30.0) or [C] to [A] (ΔOFV = - 35.7). Together, these results reveal linear IBW-based parameter scaling to be superior to either of the fixed TBW-based scaling approaches explored in this bevacizumab pediatric pharmacokinetic analysis.

### Assessment of Pharmacokinetic/Wound Healing Relationships

Twenty-six of the 27 patients with bevacizumab pharmacokinetic data were included in the analysis to determine possible associations between bevacizumab exposure and wound complications. One patient was excluded from this analysis because the family refused surgery. All patients had extremity tumors. Limb sparing surgery was performed in 20 patients and amputation in 6. Wound complications were graded utilizing prospectively defined protocol criteria (see Supplementary Material). A complication was either minor or major based on whether it was superficial (above the fascia) or deep (below the fascia). Only wound complications possibly, probably, or definitely related to bevacizumab were considered in the analysis. Six patients had major wound complications after surgery, of which 5 were determined to be related to bevacizumab therapy. Four of these 5 major wound complications occurred prior to any additional bevacizumab therapy after surgery, and the median time to occurrence of the major wound complication in these four patients was 23 days (range: 20-24). Six patients had only minor wound complications after surgery, of which only one was prior to receiving any additional bevacizumab after surgery. Because only one patient had a minor wound complication before subsequent bevacizumab therapy no formal statistical analysis was performed assessing effect of bevacizumab exposure on minor wound healing complications.

Univariate logistic regression analysis showed a significant association between $AUC_{5–surgery}$ and major wound healing complications occurring prior to any subsequent dose of bevacizumab after surgery (Fig. 4A; $p = 0.03$). The odds of a major wound complication increased to 3.1-fold (95% CI: 1.1-9.1) for every 1000 μg/ml*day increase in $AUC_{5–surgery}$. One of the children in this study who had a major wound healing complication, a 12-year old boy with a BMI of 40.6 $kg/m^2$, also had the highest estimated bevacizumab $AUC_{5–surgery}$. Simulations (Fig. 4B) indicate that his $AUC_{5–surgery}$ would likely have fallen in the middle $50^{th}$ percentile of those patients that experienced no wound complications had he been administered bevacizumab by an IBW-based dosing regimen.

## Discussion

This is the first comprehensive population pharmacokinetic/pharmacodynamic study of bevacizumab in children. Our analysis confirms the disposition of bevacizumab in children is similar to that found in adults, though the terminal half-life is slightly shorter in children. The data suggest that the incidence of major wound complications is related to bevacizumab exposure in the weeks preceding surgery, and secondly, bevacizumab exposure scales linearly with ideal body weight, rather than total body weight.

To date, only one published study has explored bevacizumab pharmacokinetics in children (22). In that study, non-compartmental analysis of the pediatric Phase I trial data showed a median (range) terminal half-life of bevacizumab in children of approximately 11.8 days (3.9 to 14.6 days), consistent with the median (range) in the present analysis of 12.2 days (8.6 to 32.4 days). The median (range) bevacizumab clearance from the same Phase I trial was 4.1 ml/day/kg (3.1 to 15.5 ml/day/kg), also very similar to the median (range) reported in the present analysis, 4.8 ml/day/kg (2.4 to 7.5 ml/day/kg). The most complete pharmacokinetic information for bevacizumab to date originates from data pooled from 491

adult patients with solid tumors on two Phase I, four Phase II, and two Phase III trials who received bevacizumab dosages of 1 to 20 mg/kg, weekly to every 3 weeks (20, 21). In that population analysis, the average terminal (β) half-life was 22.8 days with post-hoc estimates ranging from 13 to 45 days. The adult systemic clearance of bevacizumab was 0.207 to 0.264 L/day (4.6% CV). Assuming a typical adult body weight of 74 kg, this estimate falls somewhere in the range of ~2.8-3.6 ml/day/kg, so overall, the bevacizumab pharmacokinetic parameters derived from our analysis confirm prior published data in children with elimination estimates slightly more rapid than published adult data.

In adults, the clearance and volume of distribution of the central compartment were higher in males than females. In addition, the final adult population pharmacokinetic model included several covariates on clearance: gender, TBW, albumin levels, ALKP, AST, and chemotherapy. Gender, TBW, and albumin levels were also identified as significant covariates on the bevacizumab volume of distribution in adults. In contrast to these adult findings, our analysis, performed on the weight-normalized pharmacokinetic parameters for children (model parameterization [B]), identified BMI% as the most important covariate, with individual *post hoc* estimates for $V_{normalized}$ (Fig. 2) and CL significantly higher in obese children compared to normal-weight and under-weight children. The apparent explanation for this phenomenon is evident in the non-linear relationship between TBW and $V_{non\text{-}normalized}$ (Fig. 3B). This non-linearity is especially evident in pediatric patients who have age- and gender-adjusted BMI% values in percentiles generally associated with overweight/obesity (Figs. 2 and 3B).

Current bevacizumab dosing regimens in children (and adults) assume a linear relationship between volume of distribution and total body weight (i.e., model parameterization [B]). We find that IBW, by contrast, shows a strong linear relationship with bevacizumab $V_{non\text{-}normalized}$ (Fig.3C; model parameterization [C]). These results suggest that IBW-based dosing of bevacizumab would decrease the interindividual variability in exposure by at least 10% in the average patient and up to 45% in obese patients and, in turn, help to maintain more consistent serum concentrations across the spectrum of clinical BMI% values observed in our population. The dosing of several other agents with similar physicochemical properties (e.g., immunoglobulins for immunodeficiency disorders, antimicrobials, and anesthetic drugs) are also based on corrected estimates of body size such as lean body mass, AIBW, and IBW (36-39), and it is well established that extravascular distribution of large hydrophilic drugs such as proteins and other therapeutic macromolecules is limited by their permeability across biological barriers. As a result, such agents are presumably less likely to diffuse into adipose tissue and therefore more likely to scale with measures of extracellular fluid volume (ECV) or total body water (40). In children, lean body mass shows a strong positive linear correlation with measured ECV that is similar to that observed in adults (41).

Minimizing interindividual variability in bevacizumab exposure is critical to ensure therapeutic exposures are attained while mitigating drug-related adverse events. This is highlighted by the evident correlation between bevacizumab exposure and risk of major wound healing complication events observed in our patient population. Whereas previous studies have suggested an association between bevacizumab administration and surgical complications, this is the first study to our knowledge to link bevacizumab exposure directly

with wound healing outcomes. Obese patients may be inherently predisposed to wound healing complications (42, 43), but the added burden of elevated concentrations of an anti-angiogenic agent likely exacerbates the likelihood of such complications. Thus, based on the relationship between bevacizumab AUC, obesity, and incidence of wound healing complications, bevacizumab dosing scaled linearly to IBW provides an improved dosing model in children. The biologic rationale suggests a similar dosing strategy would be appropriate in adult populations, but further studies will be required to confirm if this is, in fact, true.

In summary, our data provide the first comprehensive description of the pharmacokinetics of bevacizumab in children, and shows that the terminal half-life of bevacizumab is shorter than in adults. Importantly, in patients with osteosarcoma receiving bevacizumab plus standard chemotherapy, we found that the incidence of major wound healing complications after definitive surgery of the primary tumor is correlated with bevacizumab systemic exposure prior to surgery, and bevacizumab systemic exposure scales linearly with ideal body weight. Thus, the results of this study support dosing bevacizumab based on ideal body weight in this patient population.

## Supplementary Material

Refer to Web version on PubMed Central for supplementary material.

## Acknowledgments

We would like to thank all of the patients and their families, research nurses and clinical and laboratory personnel, study coordinators, and operations staff at St. Jude Children's Research Hospital, Sidney Kimmel Comprehensive Cancer Center at Johns Hopkins, and Rady Children's Hospital who participated in this study.

**Grant Support**

This research is supported in part by Cancer Center Support CORE Grant P30 CA 21765 from the National Cancer Institute, the American Lebanese Syrian Associated Charities, and Genentech, Inc.

## References

1. Papadopoulos N, Martin J, Ruan Q, Rafique A, Rosconi MP, Shi E, et al. Binding and neutralization of vascular endothelial growth factor (VEGF) and related ligands by VEGF Trap, ranibizumab and bevacizumab. Angiogenesis. 2012; 15:171–85. [PubMed: 22302382]
2. Gerber HP, Ferrara N. Pharmacology and pharmacodynamics of bevacizumab as monotherapy or in combination with cytotoxic therapy in preclinical studies. Cancer research. 2005; 65:671–80. [PubMed: 15705858]
3. Borgstrom P, Gold DP, Hillan KJ, Ferrara N. Importance of VEGF for breast cancer angiogenesis in vivo: implications from intravital microscopy of combination treatments with an anti-VEGF neutralizing monoclonal antibody and doxorubicin. Anticancer research. 1999; 19:4203–14. [PubMed: 10628376]
4. Motl S. Bevacizumab in combination chemotherapy for colorectal and other cancers. American journal of health-system pharmacy : AJHP : official journal of the American Society of Health-System Pharmacists. 2005; 62:1021–32. [PubMed: 15901587]
5. Kabbinavar F, Hurwitz HI, Fehrenbacher L, Meropol NJ, Novotny WF, Lieberman G, et al. Phase II, randomized trial comparing bevacizumab plus fluorouracil (FU)/leucovorin (LV) with FU/LV alone in patients with metastatic colorectal cancer. J Clin Oncol. 2003; 21:60–5. [PubMed: 12506171]

6. Hurwitz H, Fehrenbacher L, Novotny W, Cartwright T, Hainsworth J, Heim W, et al. Bevacizumab plus irinotecan, fluorouracil, and leucovorin for metastatic colorectal cancer. N Engl J Med. 2004; 350:2335–42. [PubMed: 15175435]
7. Kabbinavar FF, Hambleton J, Mass RD, Hurwitz HI, Bergsland E, Sarkar S. Combined analysis of efficacy: the addition of bevacizumab to fluorouracil/leucovorin improves survival for patients with metastatic colorectal cancer. Journal of clinical oncology : official journal of the American Society of Clinical Oncology. 2005; 23:3706–12. [PubMed: 15867200]
8. Hurwitz H, Fehrenbacher L, Novotny W, Cartwright T, Hainsworth J, Heim W, et al. Bevacizumab plus irinotecan, fluorouracil, and leucovorin for metastatic colorectal cancer. The New England journal of medicine. 2004; 350:2335–42. [PubMed: 15175435]
9. Hochster HS, Hart LL, Ramanathan RK, Childs BH, Hainsworth JD, Cohn AL, et al. Safety and efficacy of oxaliplatin and fluoropyrimidine regimens with or without bevacizumab as first-line treatment of metastatic colorectal cancer: results of the TREE Study. Journal of clinical oncology : official journal of the American Society of Clinical Oncology. 2008; 26:3523–9. [PubMed: 18640933]
10. Giantonio BJ, Catalano PJ, Meropol NJ, O'Dwyer PJ, Mitchell EP, Alberts SR, et al. Bevacizumab in combination with oxaliplatin, fluorouracil, and leucovorin (FOLFOX4) for previously treated metastatic colorectal cancer: results from the Eastern Cooperative Oncology Group Study E3200. Journal of clinical oncology : official journal of the American Society of Clinical Oncology. 2007; 25:1539–44. [PubMed: 17442997]
11. Johnson DH, Fehrenbacher L, Novotny WF, Herbst RS, Nemunaitis JJ, Jablons DM, et al. Randomized phase II trial comparing bevacizumab plus carboplatin and paclitaxel with carboplatin and paclitaxel alone in previously untreated locally advanced or metastatic non-small-cell lung cancer. J Clin Oncol. 2004; 22:2184–91. [PubMed: 15169807]
12. Yang JC, Haworth L, Sherry RM, Hwu P, Schwartzentruber DJ, Topalian SL, et al. A randomized trial of bevacizumab, an anti-vascular endothelial growth factor antibody, for metastatic renal cancer. The New England journal of medicine. 2003; 349:427–34. [PubMed: 12890841]
13. Burger RA, Sill MW, Monk BJ, Greer BE, Sorosky JI. Phase II trial of bevacizumab in persistent or recurrent epithelial ovarian cancer or primary peritoneal cancer: a Gynecologic Oncology Group Study. Journal of clinical oncology : official journal of the American Society of Clinical Oncology. 2007; 25:5165–71. [PubMed: 18024863]
14. Vredenburgh JJ, Desjardins A, Herndon JE 2nd, Marcello J, Reardon DA, Quinn JA, et al. Bevacizumab plus irinotecan in recurrent glioblastoma multiforme. J Clin Oncol. 2007; 25:4722–9. [PubMed: 17947719]
15. Gutin PH, Iwamoto FM, Beal K, Mohile NA, Karimi S, Hou BL, et al. Safety and efficacy of bevacizumab with hypofractionated stereotactic irradiation for recurrent malignant gliomas. International journal of radiation oncology, biology, physics. 2009; 75:156–63.
16. Nghiemphu PL, Liu W, Lee Y, Than T, Graham C, Lai A, et al. Bevacizumab and chemotherapy for recurrent glioblastoma: a single-institution experience. Neurology. 2009; 72:1217–22. [PubMed: 19349600]
17. Kaya M, Wada T, Akatsuka T, Kawaguchi S, Nagoya S, Shindoh M, et al. Vascular endothelial growth factor expression in untreated osteosarcoma is predictive of pulmonary metastasis and poor prognosis. Clinical cancer research : an official journal of the American Association for Cancer Research. 2000; 6:572–7. [PubMed: 10690541]
18. Lee YH, Tokunaga T, Oshika Y, Suto R, Yanagisawa K, Tomisawa M, et al. Cell-retained isoforms of vascular endothelial growth factor (VEGF) are correlated with poor prognosis in osteosarcoma. Eur J Cancer. 1999; 35:1089–93. [PubMed: 10533453]
19. Kaya M, Wada T, Kawaguchi S, Nagoya S, Yamashita T, Abe Y, et al. Increased pre-therapeutic serum vascular endothelial growth factor in patients with early clinical relapse of osteosarcoma. British journal of cancer. 2002; 86:864–9. [PubMed: 11953816]
20. Lu JF, Bruno R, Eppler S, Novotny W, Lum B, Gaudreault J. Clinical pharmacokinetics of bevacizumab in patients with solid tumors. Cancer Chemother Pharmacol. 2008; 62:779–86. [PubMed: 18205003]
21. Genentech I. Center for Drug Evaluation and Research Approval Package For: Application Number STN-125085/0. 2004

22. Glade Bender JL, Adamson PC, Reid JM, Xu L, Baruchel S, Shaked Y, et al. Phase I trial and pharmacokinetic study of bevacizumab in pediatric patients with refractory solid tumors: a Children's Oncology Group Study. J Clin Oncol. 2008; 26:399–405. [PubMed: 18202416]
23. van der Bilt JD, Borel Rinkes IH. Surgery and angiogenesis. Biochimica et biophysica acta. 2004; 1654:95–104. [PubMed: 14984770]
24. Ellis LM, Curley SA, Grothey A. Surgical resection after downsizing of colorectal liver metastasis in the era of bevacizumab. J Clin Oncol. 2005; 23:4853–5. [PubMed: 16051943]
25. Howdieshell TR, Callaway D, Webb WL, Gaines MD, Procter CD Jr, Sathyanarayana, et al. Antibody neutralization of vascular endothelial growth factor inhibits wound granulation tissue formation. The Journal of surgical research. 2001; 96:173–82. [PubMed: 11266270]
26. Zhang F, Lei MP, Oswald TM, Pang Y, Blain B, Cai ZW, et al. The effect of vascular endothelial growth factor on the healing of ischaemic skin wounds. British journal of plastic surgery. 2003; 56:334–41. [PubMed: 12873460]
27. Roman CD, Choy H, Nanney L, Riordan C, Parman K, Johnson D, et al. Vascular endothelial growth factor-mediated angiogenesis inhibition and postoperative wound healing in rats. The Journal of surgical research. 2002; 105:43–7. [PubMed: 12069500]
28. Scappaticci FA, Fehrenbacher L, Cartwright T, Hainsworth JD, Heim W, Berlin J, et al. Surgical wound healing complications in metastatic colorectal cancer patients treated with bevacizumab. Journal of surgical oncology. 2005; 91:173–80. [PubMed: 16118771]
29. Meyers PA, Schwartz CL, Krailo M, Kleinerman ES, Betcher D, Bernstein ML, et al. Osteosarcoma: a randomized, prospective trial of the addition of ifosfamide and/or muramyl tripeptide to cisplatin, doxorubicin, and high-dose methotrexate. J Clin Oncol. 2005; 23:2004–11. [PubMed: 15774791]
30. Gehan EA, George SL. Estimation of human body surface area from height and weight. Cancer chemotherapy reports Part 1. 1970; 54:225–35. [PubMed: 5527019]
31. Ogden CL, Kuczmarski RJ, Flegal KM, Mei Z, Guo S, Wei R, et al. Centers for Disease Control and Prevention 2000 growth charts for the United States: improvements to the 1977 National Center for Health Statistics version. Pediatrics. 2002; 109:45–60. [PubMed: 11773541]
32. Koshida R, Nakashima E, Taniguchi N, Tsuji A, Benet LZ, Ichimura F. Prediction of the distribution volumes of cefazolin and tobramycin in obese children based on physiological pharmacokinetic concepts. Pharm Res. 1989; 6:486–91. [PubMed: 2762224]
33. Gundersen K, Shen G. Total body water in obesity. Am J Clin Nutr. 1966; 19:77–83. [PubMed: 5916037]
34. Traynor AM, Nafziger AN, Bertino JS Jr. Aminoglycoside dosing weight correction factors for patients of various body sizes. Antimicrob Agents Chemother. 1995; 39:545–8. [PubMed: 7726530]
35. Wang J, Pierson RN Jr. Disparate hydration of adipose and lean tissue require a new model for body water distribution in man. J Nutr. 1976; 106:1687–93. [PubMed: 993849]
36. Provan, D.; Nokes, TJ.; Agrawal, S.; Winer, J.; Wood, P. Clinical guidelines for immunoglobulin use. Department of Health Publication; London: 2008.
37. Han PY, Duffull SB, Kirkpatrick CM, Green B. Dosing in obesity: a simple solution to a big problem. Clin Pharmacol Ther. 2007; 82:505–8. [PubMed: 17952107]
38. Polotsky HN, Polotsky AJ. One size may not fit all: pondering antibiotic dosing in obesity. Maturitas. 2010; 66:381–2. [PubMed: 20356691]
39. Martin JH, Saleem M, Looke D. Therapeutic drug monitoring to adjust dosing in morbid obesity - a new use for an old methodology. British journal of clinical pharmacology. 2012; 73:685–90. [PubMed: 22129454]
40. Kendrick JG, Carr RR, Ensom MH. Pharmacokinetics and drug dosing in obese children. The journal of pediatric pharmacology and therapeutics : JPPT : the official journal of PPAG. 2010; 15:94–109. [PubMed: 22477800]
41. Foster BJ, Platt RW, Zemel BS. Development and validation of a predictive equation for lean body mass in children and adolescents. Annals of human biology. 2012; 39:171–82. [PubMed: 22621754]

42. Wilson JA, Clark JJ. Obesity: impediment to postsurgical wound healing. Advances in skin & wound care. 2004; 17:426–35. [PubMed: 15492679]

43. Wagner IJ, Szpalski C, Allen RJ Jr, Davidson EH, Canizares O, Saadeh PB, et al. Obesity impairs wound closure through a vasculogenic mechanism. Wound repair and regeneration : official publication of the Wound Healing Society [and] the European Tissue Repair Society. 2012; 20:512–22.

## Translational Relevance

Though not yet approved for use in children, bevacizumab is a widely studied antiangiogenic agent in adults, and several early phase trials are currently evaluating bevacizumab regimens in children. This report describes the only population pharmacokinetic model of bevacizumab in children and establishes, for the first time, bevacizumab pediatric pharmacokinetic parameters including the interindividual and interoccasion variability. This pharmacokinetic/pharmacodynamic analysis also demonstrates a significant link between treatment outcomes (i.e., postsurgical wound healing) and systemic bevacizumab exposure in children and adolescents treated for osteosarcoma. The impact of this finding is clinically significant because surgical tumor resection is an important component of care for patients suffering from osteosarcoma and many other solid tumor types. Pharmacokinetic simulations suggest that dosing of bevacizumab based on ideal body weight would be more appropriate to mitigate pharmacokinetic variability encountered due to discrepancies in body composition between underweight and overweight children and adolescents.

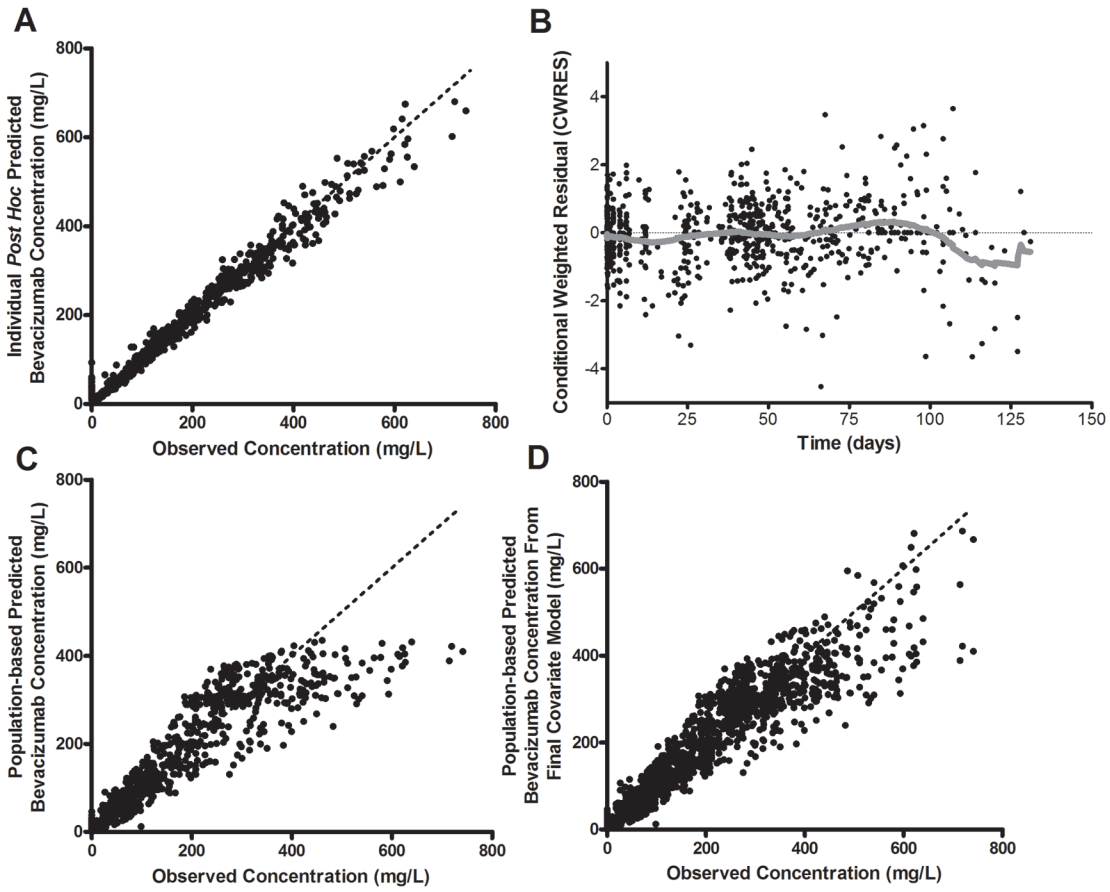


**Figure 1.**

Goodness-of-fit plots from the bevacizumab population pharmacokinetic model (model parameterization [B]). A, Observed versus individual predicted concentrations for the covariate-free (base structural) model. B, Conditional weighted residual (CWRES) versus time in days for the covariate-free model with LOWESS (solid line). C, Observed versus population predicted concentrations for the covariate-free model. D, Observed versus population predicted concentrations for the final population model. Dashed lines in panel A, C, and D represent the line of unity.

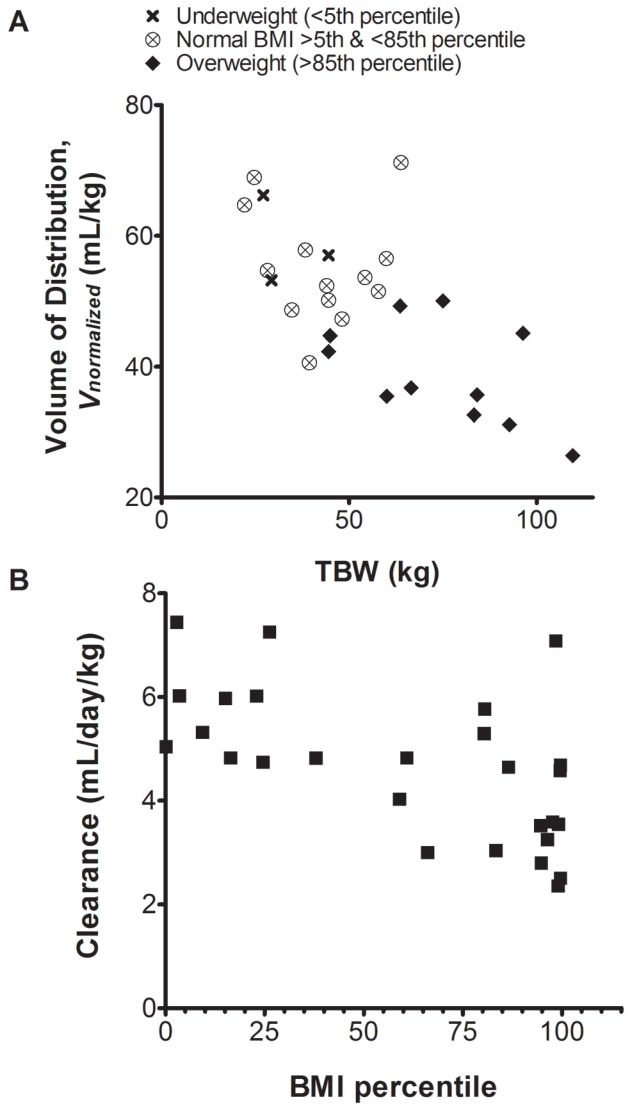


**Figure 2.**

A, The plot of bevacizumab $V_{normalized}$ (weight normalized volume of distribution from parameterization [B]) versus total body weight (TBW) implies an apparent non-linear relationship between TBW and $V_{non\text{-}normalized}$. In cases of extreme body weight, the $V_{normalized}$ of bevacizumab was up to 53% lower (BMI > 97$^{th}$ percentile) or up to 32.1% higher (BMI < 3$^{rd}$ percentile) than the population median value. B, The trend in the scatterplot of CL versus BMI percentile further confirms that body composition is a key determinant of pharmacokinetic interindividual variability when bevacizumab is dosed on a TBW-based regimen.

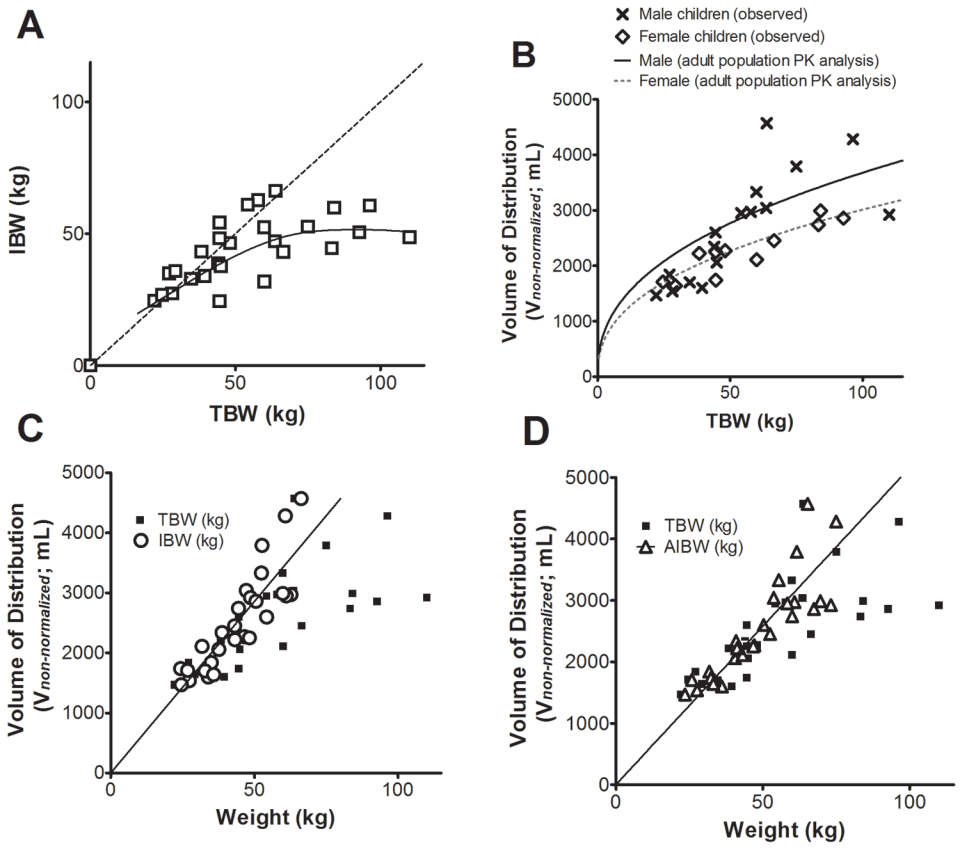


**Figure 3.**

A, The ideal body weight (IBW) per unit total body weight (TBW) decreases with increasing TBW. The dashed line represents the line of unity and the solid line represents a smooth through the data points (n=27). B, Volume of distribution (non-weight normalized from parameterization [C]) estimates versus TBW (n=27) overlaid with the gender-specific volume versus TBW relationships derived previously in the pooled adult dataset (solid line corresponding to adult males and the dashed line corresponding to adult females) (21). The data indicates that the body weight to volume of distribution relationship is similar between children studied in this population and the adult population. C, The volume of distribution (posthoc estimates using the base structural non-normalized parameters from parameterization [C]; mL) versus TBW (filled squares) and IBW (open circles) indicates that excess body weight associated with obesity accounts for a large amount of the non-linearity ($r^2 = 0.752$ for IBW linear regression). D, volume of distribution (posthoc estimates using the base structural non-normalized parameters from parameterization [C]; mL) versus TBW (filled squares) and adjusted body weight (AIBW) (open triangles) shows a similar trend as in panel C ($r^2 = 0.746$ for AIBW linear regression).

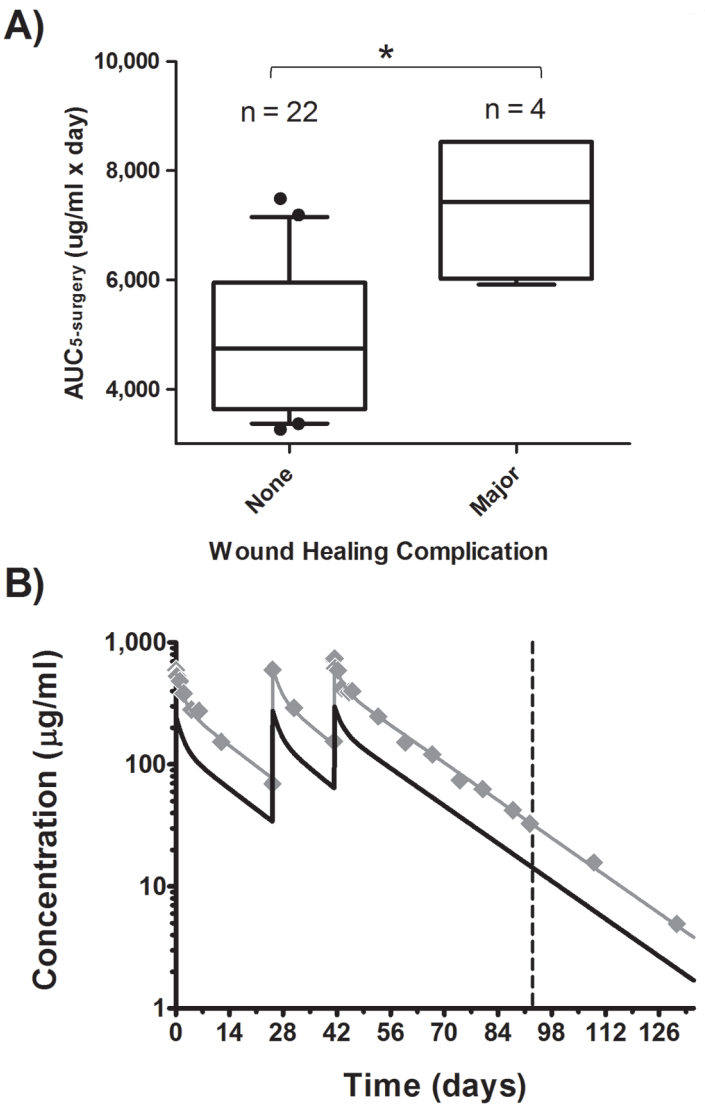


**Figure 4.**

A, The odds of a major wound complication increased by 3.1-fold (*95% CI: 1.1-9.1; $p$ = 0.03) for every 1000 µg/ml*day increase in $AUC_{5–surgery}$ (box: interquartile range; whiskers: 90% CI; filled circles: data residing outside 90% CI). In B, observed bevacizumab concentration-time data (filled diamonds) are shown for an obese 12-year old boy with a BMI of 40.6 kg/$m^2$ who experienced a major wound healing complication (surgery on day 93; vertical dashed line). Pharmacokinetic simulations indicate that 15 mg/kg IBW-based dosing (solid black line) decreases bevacizumab $AUC_{5–surgery}$ from 8,529 µg/ml*day to 3,756 µg/ml*day compared to simulation using the actual body weight dosing (solid gray line), effectively reducing the odds of major wound complication by almost 300-fold for this child.

## Table 1

Summary of Patient Characteristics and Laboratory Data

| **Total Number of Patients** | **27** |
|---|---|
| **Sex** | |
| Male:Female | 16:11 |
| **Race** | |
| White:Black:Other* | 15:9:3 |
| **Stage** | |
| Localized:Metastatic | 21:6 |
| **Age (years)** | |
| Median (range) | 12.2 (6.8 – 18.1) |
| Mean (SD) | 12.3 (3.2) |
| **Height (centimeters)** | |
| Median (range) | 154.0 (126.0 – 179.0) |
| Mean (SD) | 153.9 (15.5) |
| **Weight (kilograms)** | |
| Median (range) | 48.1 (22.1 – 110.0) |
| Mean (SD) | 54.9 (23.4) |
| **Body Surface Area ($m^2$)** | |
| Median (range) | 1.45 (0.89 – 2.27) |
| Mean (SD) | 1.52 (0.38) |
| **BMI percentile (%)** | |
| Median (range) | 80.3 (0.1 – 99.6) |
| Mean (SD) | 61.2 (37.8) |
| **TP (g/dL)** | |
| Median (range) | 7.5 (5.9 – 8.0) |
| Mean (SD) | 7.3 (0.6) |
| **ALKP (IU/L)** | |
| Median (range) | 252 (124 – 550) |
| Mean (SD) | 261 (111) |
| **AST (IU/L)** | |
| Median (range) | 22 (15 – 40) |
| Mean (SD) | 25.2 (7.4) |
| **Albumin (g/dL)** | |
| Median (range) | 3.8 (2.8 – 4.4) |
| Mean (SD) | 3.9 (0.4) |

[*] Hispanic (2); Asian (1)

Abbreviations: SD, standard deviation; TP, total protein; ALKP, alkaline phosphatase; AST, aspartate aminotransferase; BMI, body mass index.

## Table 2

Final Population Pharmacokinetic Parameter Median Estimates and Confidence Interval from 1,000 Bootstrap Replicates of Original Dataset

| Parameter/Covariate Relationship | Median Estimate (95% CI) | Inter-Individual Variability, % CV [a] (95% CI) | Inter-Occasion Variability, % CV [b] (95% CI) |
|---|---|---|---|
| CL (mL/day/kg) = $\theta_{CL} \times e^{BMI\% \times \theta_{BMI\%,CL}}$ | | | |
| $\theta_{CL}$ | 5.16 (4.36 – 5.74) | 18.4 % (8.4 – 33.9 %) | 18.2 % (13.3 – 22.6 %) |
| $\theta_{BMI\%,CL}$ | -0.004 (-0.006 – -0.002) | | |
| $V_{normalized}$ (L/kg) = $\theta_V \times e^{BMI\% \times \theta_{BMI\%,V}}$ | | | |
| $\theta_V$ | 62.7 (57.5 – 69.0) | 13.2 % (9.0 – 17.6 %) | 4.7 % (1.6 – 7.4 %) |
| $\theta_{BMI\%,V}$ | -0.005 (-0.006 – -0.003) | | |
| $k_{12}$ ($hr^{-1}$) | 0.222 (0.187 – 0.268) | 25.0 % (12.7 – 37.3 %) | --- |
| $k_{21}$ ($hr^{-1}$) | 0.335 (0.250 – 0.418) | 49.8 % (15.1 – 87.7 %) | --- |
| Residual variability | | | |
| Proportional | 0.014 (0.004 – 0.018) | --- | --- |
| Additive | 0.003 (-0.003 – 0.010) | --- | --- |

*CL*: clearance, $V_{normalized}$ : volume of central compartment, $k_{12}$ and $k_{21}$: inter-compartmental rate constants,

[a] $\sqrt{\omega^2} \times 100\%$ and

[b] $\sqrt{\phi^2} \times 100\%$ (both from equation 1), BMI%: body mass index percentile